Available online at www.sciencedirect.com
SCIENCE DIRECT®
Pergamon
Acta Materialia 51 (2003) 3675–3686
Acta MATERIALIA
www.actamat-journals.com

The relative free energies of grain boundaries in magnesia as a function of five macroscopic parameters

David M. Saylor [a, 1], Adam Morawiec [b], Gregory S. Rohrer [a,*]

[a] *Materials Science and Engineering Department, Carnegie Mellon University, Pittsburgh, PA 15213, USA*
[b] *Institute of Metallurgy and Materials Science, Polish Academy of Sciences, Cracow, Poland*

Received 2 December 2002; accepted 21 March 2003

Abstract

Using measurements of the geometric and crystallographic characteristics of approximately 10^4 triple junctions in a MgO polycrystal, the relative grain boundary energy has been determined as a function of five macroscopic parameters. The relative energy of a particular grain boundary is inversely correlated with its frequency of occurrence. At all misorientations, grain boundaries with {1 0 0} interface planes have relatively low energies. For low misorientation angle grain boundaries, the results are consistent with the predictions of dislocation models. At high misorientation angles, the population and energy are correlated to the sum of the energies of the free surfaces that comprise the boundary.

Keywords: Grain boundary energy; Ceramics; Microstructure; Dislocation boundaries; Coincident lattices

1. Introduction

Grain boundaries in materials with centrosymmetric crystal structures can be distinguished on the basis of five macroscopically observable parameters [1]. Three parameters are needed to specify the transformation that brings two adjacent misoriented crystals into coincidence; the remaining parameters specify the orientation of the boundary plane separating the crystals. Based on measurements of dihedral angles at triple junctions where three grain boundaries meet [2–6] or at thermal grooves where a grain boundary meets a free surface [7–14], it has been shown that the grain boundary free energy per unit area varies with the macroscopically observable parameters. However, the relative grain boundary energy has not yet been measured as a function of all five degrees of freedom. The basic problem is that there are so many physically distinct boundaries in the five-dimensional domain that if one applies traditional microscopies under human control, it was not feasible to make enough dihedral angle measurements to characterize all of the distinguishable interfaces.

In a companion paper referred to as Part I, an experimental method was described for mapping

* Corresponding author. Tel.: +1-412-268-2696; fax: +1-412-268-3113.
E-mail address: gr20@andrew.cmu.edu (G.S. Rohrer).
[1] Present address: National Institute of Standards and Technology, Gaithersburg, MD, USA.

1359-6454/03/$30.00
doi:10.1016/S1359-6454(03)00182-4

the geometry of the grain boundary network and measuring the frequency with which different types of grain boundaries occur [15]. This semi-automated technique has been applied to MgO and was used to measure the grain boundary dihedral angles of 1.9×10^4 triple junctions assumed to be in local thermodynamic equilibrium; these measurements are used here to determine the grain boundary energies. Thus, the purpose of the present paper is to report on the relative grain boundary energy of MgO as a function of the five macroscopic grain boundary parameters. After describing the methods for determining the relative energies in the next section, the characteristics of the five-dimensional energy distribution are presented in Section 3. In Section 4, the observed energies are compared to existing models for the anisotropy of the grain boundary energy and our findings are summarized in Section 5.

2. Methods

2.1. Sample

The polycrystalline magnesia sample has been described in Part I [15]. As part of the earlier analysis, we measured the function $\lambda(\Delta g, \mathbf{n})$, which is the relative frequency of occurrence of a grain boundary with misorientation (Δg) and boundary plane normal ($\mathbf{n}$), in units of multiples of a random distribution (MRD). These data serve as a basis for the present analysis, whose goal is to determine $\gamma(\Delta g, \mathbf{n})$, the relative grain boundary energy per unit area as a function of misorientation and boundary plane normal. It is important to recognize that the grain boundary dihedral angles were established during a 48 h high temperature anneal in air at 1600 °C and that before analysis, the surface region was removed by grinding. Thus, the energies that we extract from these data are representative of the local thermodynamic equilibrium at this temperature, in the bulk region of the sample. Although grain boundary positions were identified by observations of grain boundary grooves formed on a polished plane by a shorter anneal at 1400 °C, there is no evidence for grain boundary migration during this lower temperature treatment.

2.2. Triple junction geometry data

The triple junction geometries were extracted from the previously described grain boundary network data assembled from five adjacent parallel sections through the microstructure [15]. Points where the same triple line intersects adjacent layers were identified by comparing the lateral positions of the points and the orientations of the three grains bounding the triple junctions on each layer. Based on the lateral offset of the junction positions and the spacing between the two sections (Δh), the triple line direction ($\mathbf{l}$) was determined (see Fig. 1). Taking the grain boundary tangents ($\mathbf{t}_i$) directly from the planar sections, it was possible to determine the grain boundary plane normal ($\mathbf{n}_i = \mathbf{l} \times \mathbf{t}_i$). Because of boundary curvature and experimental uncertainties, the apparent grain boundary tangents are not necessarily identical on adjacent layers. To average out the effect of these differences, the geometry of each triple junction was determined twice; once using the boundary tangents in the top layer and a second time using the tangents observed in the bottom layer. Thus, each valid triple junction was considered twice in our analysis and this produces the set of 19,094 observed triple junctions.

2.3. Energy reconstruction

The key assumption underpinning this and previous measurements of the relative grain boundary

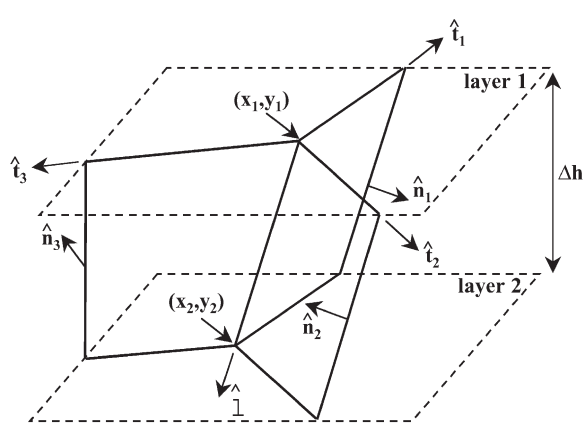

Fig. 1. Schematic representation of the geometric parameters required to characterize a grain boundary triple junction.

energy is that the interfacial junctions are in local thermodynamic equilibrium and, therefore, obey the Herring [16] condition. Under these circumstances, the relative energies can be determined using the capillarity vector reconstruction method, which is described in detail elsewhere [17]. Here, we provide a brief account of the method's underpinnings. Hoffman and Cahn [18,19] expressed the Herring condition in the following way:

$$(\xi^1 + \xi^2 + \xi^3) \times \mathbf{l} = 0, \quad (1)$$

where ξ^1, ξ^2, and ξ^3 are the capillarity vectors associated with the three grain boundaries. In general, the component of ξ perpendicular to a boundary is $\xi_\perp = \gamma(\mathbf{n})\mathbf{n}$, where $\gamma(\mathbf{n})$ is inclination dependent energy of a boundary with a given misorientation. The component of ξ parallel to the boundary, $\xi_\parallel = (\partial\gamma/\partial\beta)_{\max}\mathbf{t}_0$, points in the direction of maximum increase in $\gamma(\mathbf{n})$, where β is the right-handed angle of rotation about $\mathbf{l}$. For every observed triple junction, there is a separate equilibrium expression, as given in Eq. (1). For each such equation, we have measured $\mathbf{t}$ and $\mathbf{n}$ for each boundary and $\mathbf{l}$ for the junction. Therefore, the only unknowns are the scalar components of the three ξ vectors. If we partition the range of distinguishable grain boundaries, then there is a discrete ξ vector for each boundary type. Using an iterative procedure, it is then possible to find the set of capillarity vectors that most nearly satisfies this system of linear equations [17].

A specific type of grain boundary is distinguished by its misorientation (Δg) and its boundary plane ($\mathbf{n}$). The method used to partition the domain of grain boundary types was described in Part I [15] and the iterative procedure used to find the set of ξ that satisfy the equilibrium equations has already been described by Morawiec [17]. The relaxation factor, which controls the magnitude of changes applied to each capillarity vector during subsequent iterations, was chosen as ten times the inverse of the maximum number of equations that any one interfacial character was involved in (here, 0.0585). The iteration process was stopped when the change in the sum of the magnitude of all of the deviation vectors is less than 1% of the change during the first iteration (here, 279 steps). Because the observed grain boundary types are not distributed uniformly, some cells are poorly populated and this creates nonphysical discontinuities in the capillarity vector field. We eliminate these discontinuities after the final step by smoothing the result as follows. The value of ξ in each cell is replaced by the average of that vector and the vectors in the adjacent cells. Finally, for each grain boundary type, the energy ($\gamma\xi\cdot\mathbf{n}$) was taken as the average of all 36 symmetrically equivalent cells that correspond to the boundary type.

The capillarity vector reconstruction method was originally tested on simulated data containing 2×10^5 triple junctions [17]. Since our experimental data set contains about an order of magnitude fewer triple junctions, we have again tested the performance of the method on a smaller simulated data set. Following Ref. [17], simulated data is generated using a model function for the grain boundary energy over all five parameters that is based on a uniform energy distribution with cusps at certain misorientations, shaped by analogy to the Read–Shockley (RS) [20] expression for the energy of low angle boundaries. In the present case, the function contained one cusp at a misorientation of 60° about [1 1 1] with a boundary plane normal to [1 1 1] and another at a misorientation of 45° about [1 1 0] with a boundary plane normal to [1 1 0]. The model function also had a special cusp at zero misorientation that was independent of the boundary plane. Simulated observations from 2×10^4 triple junctions were generated using this function. To simulate experimental errors, all of the model observations were perturbed by a random angle generated from a Gaussian distribution with a standard deviation of 5°. The energy reconstruction was conducted using the same set of discrete grain boundary types, relaxation parameter, and convergence criterion as the actual measurements.

The reconstructed and model energies are compared in Fig. 2. Note that while the trends in the model function are reproduced, the magnitudes of the energy differences are not. In particular, the reconstructed energy has cusps that are more shallow than those in the model function. Based on this simulation, we conclude that the energy reconstructed from our experimental data will exhibit the

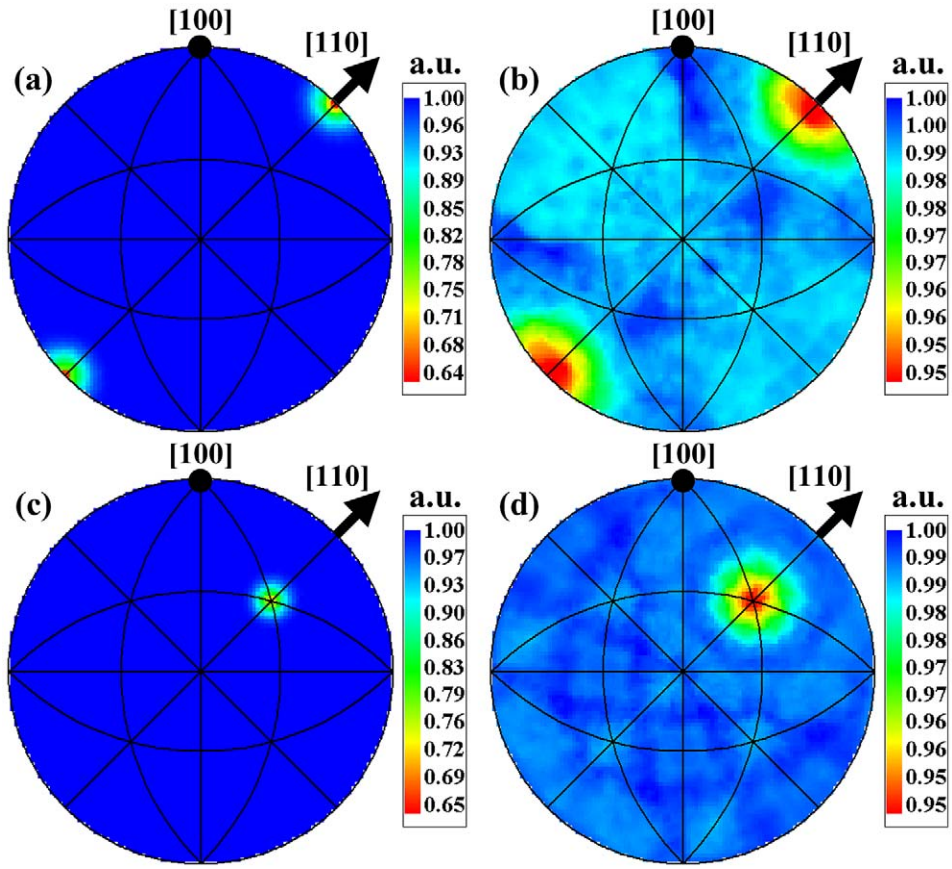

Fig. 2. (a) Model and (b) reconstructed energies for boundaries with a 45° rotation about [1 1 0]. (c) Model and (d) reconstructed energies for 60° misorientation about [1 1 1].

same qualitative features as the true function, but it will be less anisotropic.

3. Results

Results for the low angle boundaries formed by rotations about <1 1 0> are illustrated in Fig. 3. When the relative energies (a) are compared to the population (b), it is clear that there is an approximate inverse correlation between the energies and the populations. The RS [20] model predicts that the energies of grain boundaries with low angle misorientations will vary with the density and energy of the dislocations that compensate for the misfit. While the famous RS dependence of the energy on the misorientation will not be visible because of the relatively coarse discretization, the influence of the grain boundary plane on the energy is expected to be observed at a fixed misorientation. Therefore, we can determine if the RS model provides a plausible explanation for the observations in the following way.

Given a specific type of grain boundary (Δg,**n**), and three non-coplanar Burgers vectors ($\mathbf{b}_i$), Frank's [21] formula can be used to determine a density of these dislocations needed to make the boundary. In the analysis that follows, we will assume that edge and screw dislocations have the same energy per length and that the energy per unit area of the boundary is proportional to the dislocation density (ρ). Following RS [22], we calculate the vectors $\mathbf{N}_i = \mathbf{b}_i^* \times \mathbf{u} - \mathbf{n}(\mathbf{n}\cdot\mathbf{b}_i^* \times \mathbf{u})$ which are simultaneously perpendicular to the ith dislocation

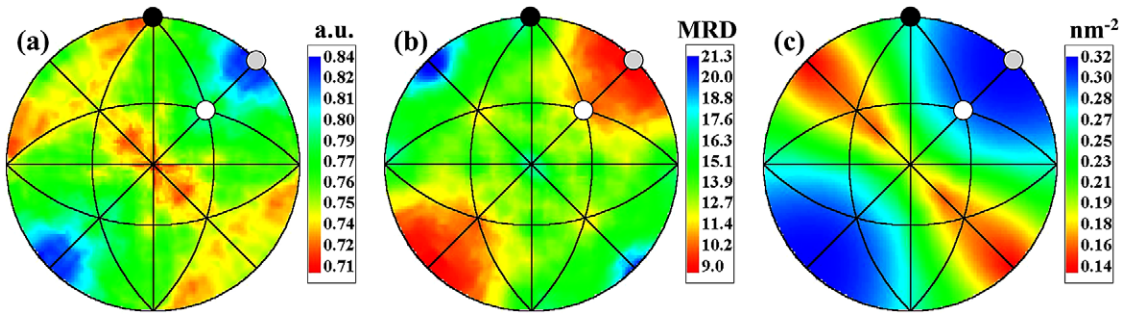

Fig. 3. (a) The reconstructed energies, (b) the observed population, and (c) geometrically necessary dislocation densities for a 5° misorientation about [1 0 1]. The quantities are plotted in stereographic projection, with the [1 0 0], [1 1 0], and [1 1 1] directions marked with a solid black, gray, and white circle, respectively.

line and the boundary plane normal (**n**). In the expression for $\mathbf{N}_i$, **u** is the misorientation axis and $\mathbf{b}_i^*$ are reciprocal vectors. For example, $\mathbf{b}_1^* = (\mathbf{b}_2 \times \mathbf{b}_3)/(\mathbf{b}_1 \cdot (\mathbf{b}_2 \times \mathbf{b}_3))$ and $\mathbf{b}_2^*$ and $\mathbf{b}_3^*$ are obtained by permuting subscripts. For small misorientation angles (θ), the magnitude of $\mathbf{N}_i$ is $1/(\theta D_i)$, where D_i is the distance between adjacent dislocation lines of the ith type. Therefore $|\mathbf{N}_i|\theta$ is the number of dislocation lines cut per length of $\mathbf{N}_i$. To get a dislocation density in the interface (ρ), we consider how many dislocations lines are cut by the three $\mathbf{N}_i$ in a circular area of interface with a unit radius, r

$$\rho = \frac{\sum_i 2r\theta \mathbf{N}_i}{\pi r^2} = \frac{2\theta}{\pi r} \sum_i \mathbf{N}_i. \tag{2}$$

In practice, we have more than one possible set of three non-coplanar dislocations, so we perform the calculations for all sets, and select the smallest density. To complete the calculation, we have to specify the types of dislocations. Based on observations of deformed magnesia [23] and other rock salt compounds [24], we assume that the boundaries are made up of dislocations of the type $\mathbf{b} = \mathbf{a}/2 < 1\,1\,0 >$. We also explored the possibility that dislocations with $\mathbf{b} = \mathbf{a}/2 < 1\,0\,0 >$ could contribute to boundary formation. However, the non-coplanar sets of dislocations with the minimum density for each boundary never contained this second type of dislocation.

The result of this calculation for a 5° misorientation around the [1 1 0] axis is shown in Fig. 3c. The minimum dislocation density occurs for tilt boundaries with $(\bar{1}\ 1\ 0)$ and $(1\ \bar{1}\ 0)$ planes. Within the resolution of our partitioning scheme, these are indistinguishable from symmetric tilt boundaries (the ideal symmetric case has **n** inclined from $(\bar{1}\ 1\ 0)$ and $(1\ \bar{1}\ 0)$ by 2.5°). These orientations are also positions of relatively low energy (Fig. 3a) and high population (Fig. 3b) in the experimental data. The highest dislocation densities are found for the pure twist boundaries on (1 1 0) and $(\bar{1}\ \bar{1}\ 0)$ planes, positions of maximum energy and minimum population.

Fig. 4 shows the relative energies of grain boundaries with misorientations of 10°, 20°, and 30° around the [1 1 0] axis. In each case, the energies are relatively low for boundaries with planes near {1 0 0} orientations. If one compares these results to the grain boundary populations for the same boundaries (for example, compare Fig. 8a in part I with Fig. 4b in the present paper), there is an obvious inverse correlation. Boundary plane orientations with relatively low grain boundary energy correspond to orientations with relatively high populations near {1 0 0} and the higher energy orientations have relatively low populations. To illustrate that these relationships persist throughout the data set, we compare all boundaries in a fixed range of energy to the population of each type of boundary (λ) and to the minimum inclination of the boundary normal from the <1 0 0> direction (θ_{100}). For this comparison, we consider the boundary types corresponding to the center of the cells in the five parameter space. After discretizing the range of energies into equal partitions, we

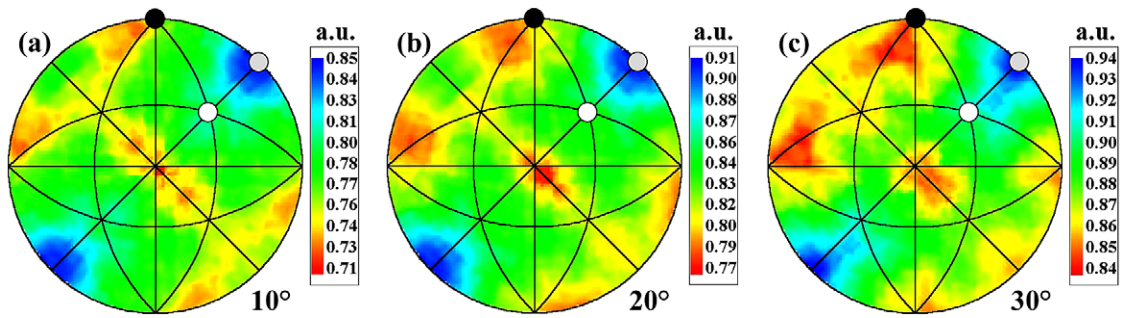

Fig. 4. The reconstructed energies for boundaries with misorientations of (a) 10°, (b) 20°, and (c) 30° around the [1 1 0] axis. The energies, which are in arbitrary units (a.u.), are plotted in stereographic projection.

determined the mean and standard deviation of $\ln(\lambda + 1)$ and θ_{100} for all boundaries in each partition. This procedure allows us to examine the correlation over the entire space. The results illustrated in Fig. 5a show that as γ increases, θ_{100} increases and λ decreases. A second way to look at these data is to average the energy over all misorientations, and plot the dependence of this misorientation averaged energy as a function of boundary plane, as in Fig. 5b. While the averaging compresses the dynamic range of the data, the {1 0 0} orientations are clear minima.

To quantify the extent to which the reconstructed energy function correlates to the distribution, we use the Spearman rank-order correlation coefficient, r_s [25]. The values of r_s range from -1 to 1, which indicate perfect negative and positive correlation, respectively, and for $r_s = 0$, no correlation exists. The comparison is based on values of the distribution ($\lambda(\Delta g, \mathbf{n})$) that correspond to the center of each cell in the parameter space. Comparing the reconstructed energies to the frequency of occurrence of each type, we find an r_s equal to –0.77; this indicates a high degree of (negative) correlation and a marked relationship between the two distributions [26]. It should be noted that this strong negative correlation arises principally from the three misorientation parameters. In other words, if we average over the boundary planes and compare the population and the misorientation dependence of the reconstructed energies, the correlation rises to a remarkably high value of $r_s = -0.98$. On the other hand, if we examine the correlation over only the two inclination parameters by

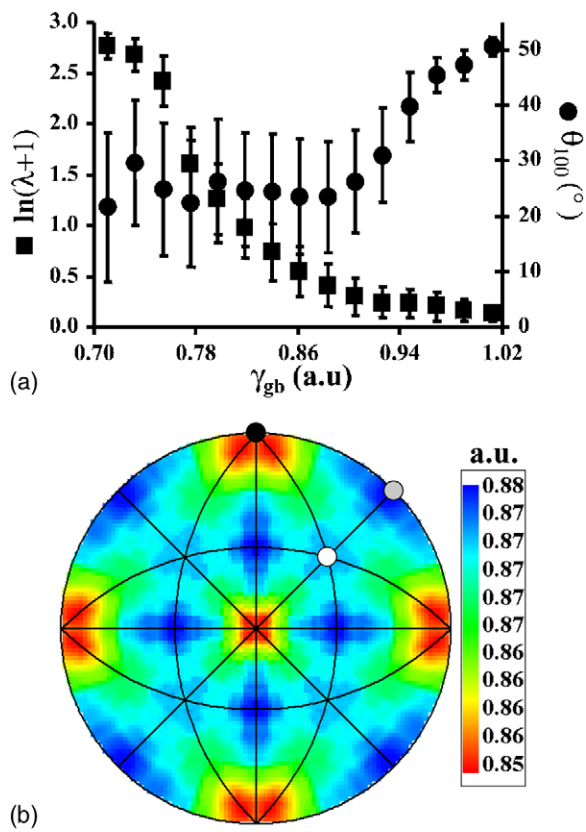

Fig. 5. (a) The grain boundary population (squares) and the minimum inclination of the boundary normal from a <1 0 0> direction (circles) plotted as a function of the reconstructed grain boundary energy. For each quantity, the average of all values within a range of 0.022 a.u. is represented by the point; the bars indicate one standard deviation above and the mean. (b) The misorientation averaged reconstructed grain boundary energies plotted in stereographic projection.

comparing the reconstructed energies to normalized values of the distribution ($\lambda(\Delta g, \mathbf{n})/\lambda(\Delta g)$), we find r_s to be –0.40, which indicates a low to moderate inverse correlation.

Our ability to determine the misorientation dependence of the energy more accurately than the inclination dependence is related both to the difference in the experimental uncertainties in measuring these parameters and to the difference in the total variance of the energy over these parameters. The estimated experimental errors in the misorientation calculation ($\leq 2°$) are significantly less than the size of partitions in the five-dimensional domain of distinct boundary types (~10°). On the other hand, the uncertainty in the determination of the boundary plane normal can be larger than the size of the partition (the uncertainty varies with inclination from the sample normal and has a maximum value of about 15° for planes in the zone of the surface normal). Furthermore, we expect the energy to vary over a wider range of values as a function of misorientation than as a function of boundary plane orientation. Nevertheless, there is a high degree of (negative) correlation between the reconstructed relative grain boundary energies and the frequency of occurrence of specific types of boundaries over the five-parameter domain.

The data show that grain boundaries with {1 0 0} planes have lower energies and occur more commonly in this microstructure. This behavior is reminiscent of the orientation dependence of the surface energy of MgO. Earlier measurements of the surface energy anisotropy of magnesia, conducted in our laboratory on the same sample, indicated that the (1 0 0) plane has the minimum energy. The energies of the (1 1 0) and (1 1 1) surfaces are 7% and 17% higher than (1 0 0), respectively [27]. Since these relative surface energies are consistent with the increase in the density of broken bonds, we take the surface energy anisotropy of MgO to be a quantitative indicator of the extent to which the ideal bonding is disrupted by forming a particular surface.

If the grain boundary energy also reflects the local disruption in bonding, then we can create a hypothetical energy by summing of the energies of the two surfaces planes comprising the interface, and subtracting a binding energy that reflects the gain in bonds that occurs when the two surfaces are brought together to create the grain boundary [28]. For general boundaries, where the repeat units of the two free surfaces do not form a commensurate structure (i.e., there is no special coincidence relation) and the misorientation cannot be created by a set of non-overlapping dislocations, the density of reformed bonds should be more or less constant. In these cases, the binding energy should also be constant and this means that the energy anisotropy of general boundaries should be reproduced by summing the measured energies of the two free surfaces that make up the boundary. We therefore compare hypothetical boundary energies computed based only on measured surface energies to the experimental observations to test the idea that the density of broken bonds in the interface determines the grain boundary energy anisotropy.

The results in Fig. 6 compare the hypothetical energy, the measured energy, and the observed population for boundaries with 10°, 20°, and 30° of misorientation around [1 0 0]. These plots show that the anisotropy of the hypothetical grain boundary energy is correlated with the reconstructed grain boundary energy and has an inverse correlation with the grain boundary population. For {1 0 0} boundary planes, the sum of the surface energies is low, as are the reconstructed energies. The distribution, on the other hand, exhibits maxima at these positions.

To quantify the extent to which the hypothetical energy function correlates to the distribution, we again use the Spearman rank-order correlation coefficient, r_s [26]. Here it must be recognized that the hypothetical energies are expected to reproduce only the dependence of the energy on the grain boundary plane ($\gamma(\mathbf{n})$); they will not decrease systematically with misorientation angle. Therefore, we compare the hypothetical energies to the normalized values of the distribution ($\lambda(\Delta g, \mathbf{n})/\lambda(\Delta g)$) and find r_s equal to -0.76. This value also indicates a high degree of (negative) correlation.

It is noteworthy that the hypothetical energies are more strongly correlated to the inclination dependence of the grain boundary population than the reconstructed energy. As illustrated by the results in Fig. 2, the energy reconstruction pro-

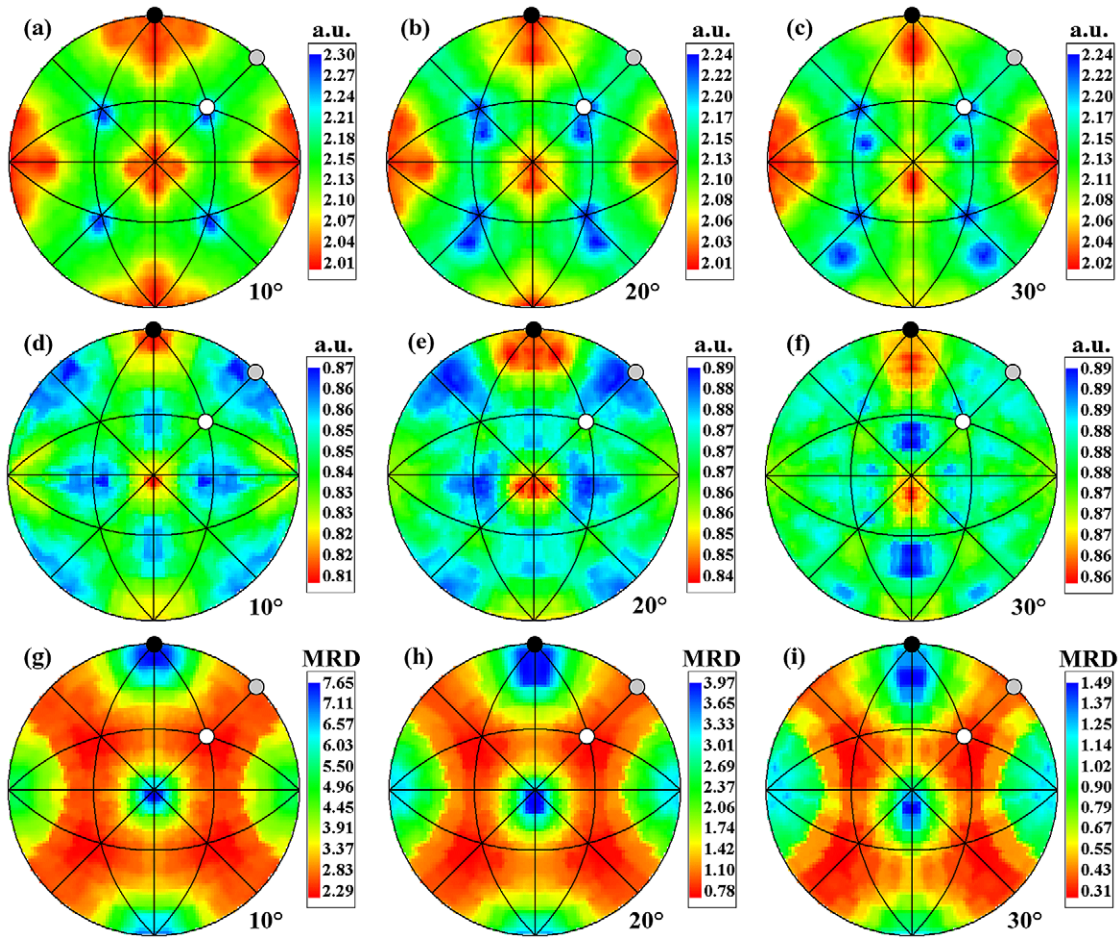

Fig. 6. The hypothetical grain boundary energies based on the surface energies at fixed misorientations corresponding to rotations about [1 0 0] of (a) 10°, (b) 20°, and (c) 30°. For comparison, the reconstructed energies (d–f) and the observed population (g–i) at the same fixed misorientations are also shown. The quantities are plotted in stereographic projection.

cedure reproduces the general trends in the model function, but underestimates the relative anisotropies. Furthermore, while the simulated data was evenly distributed in the five-dimensional space, the real data was concentrated such that for axes different from $<1\,1\,1>$, the data is sparse for rotations greater then 35°. In these poorly populated regions, the reconstructed energy is not expected to be accurate and this contributes to the lower degree of negative correlation with the inclination distribution.

4. Discussion

For the case of low misorientation angle grain boundaries, the conventional RS [20] model provides a reasonable explanation for the relatively low energy of the symmetric tilt boundaries on $(1\,\bar{1}\,0)$ and $(1\,\bar{1}\,0)$ planes. This is because in crystals with the rock salt crystal structure in general, and in MgO in particular, dislocations with Burgers vectors of $\mathbf{a}/2 < 1\,1\,0 >$ are most common. While any boundary can be formed by three

dislocations with non-coplanar Burgers vectors, boundaries with the minimum dislocation density occur when the misorientation can be created by a single set of parallel dislocations. In networks containing two or more types of dislocations, anti-parallel contributions to the displacement cancel each other so that more dislocations are required to create the same angular rotation of the lattice. The effect of this is seen most clearly in Fig. 3c, where the minimum dislocation density occurs for pure, symmetric tilt boundaries on (1 1 0) and (1 $\bar{1}$ 0) planes. In each case, the boundary can be created by a single set of parallel edge dislocations. As the plane is changed along the zone of pure tilt boundaries to orientations where the boundary is asymmetric, more and more dislocations with a second Burgers vector must be added and this systematically increases the density to a maximum when **n** is ~90° from the symmetric plane. Finally, we recall that the dislocation model applied here is based on the assumption that boundaries are formed by the minimum number of geometrically necessary dislocations. While the results in Fig. 3 indicate that this model provides a consistent explanation for the present observations, it does not rule out the possible existence of more complex microscopic defect structures.

The low energy of {1 1 0} tilt boundaries is also consistent with previous studies of crystals with the rock salt structure that have been annealed after deformation. In these cases, annealing usually leads to polygonization, where the resulting low angle grain boundaries have tilt character and most frequently lie on {1 1 0} type planes [23]. In the present case, these boundaries also dominated the population, but they appeared as a result of grain growth rather than polygonization. This is consistent with the idea that grain growth involves not only the elimination of total grain boundary area, but the elimination of the highest energy boundaries while the lower energy boundaries are preserved.

Our observations of high angle grain boundaries should be compared to the theory of the coincident site lattice (CSL), which has had a profound influence on grain boundary studies for the past three decades [29]. There is some evidence that boundaries with these special geometries have lower energies [3,4,10,12–14] and even that materials with high fractions of these boundaries have properties that are superior to materials with more random grain boundary networks [30]. However, there are also observations showing that some low Σ CSL boundaries (boundaries with high coincidence) do not have reduced energies [3,7,8,11]. While it is common practice to consider a boundary to be "special" on the basis of misorientation alone, it must be recognized that a CSL boundary only has high interface coincidence on certain coherent planes, and these are relatively rare. For example, using the discretization scheme employed here, there are 6561 distinct boundary types and fewer than 1% correspond to coherent low sigma CSL boundaries ($\Sigma \leq 19$).

The findings illustrate that in MgO, the CSL boundaries are nearly insignificant in comparison to the boundaries terminated on one side by a {1 0 0} plane. The latter boundaries comprise a far greater part of the five-dimensional space (they occur at every misorientation), they are on average populated with an equal or greater frequency, and they have lower energies. The present results seem to contradict previous observations of boundaries in MgO smoke, which have extraordinarily high fractions of low Σ CSL twist boundaries [31]. However, one must remember that grain boundaries in the present case are formed as the result of extensive grain growth. The twist boundaries found in aggregates of smoke particles are thought to arise from a nucleation process in the hot plume of burning Mg [31]. It should be noted, however, that one characteristic of the smoke aggregates is remarkably similar to the present observations: the grain boundaries in MgO smoke are always terminated on a {1 0 0} plane.

In comparing the relative importance of the CSL boundaries and the boundaries terminated by {1 0 0} planes, it is instructive to examine the energy and distribution of boundary planes at the Σ5 misorientation. Fig. 7 shows the population and energy of pure tilt Σ5 boundaries. The boundaries that couple the highest population and the lowest energy are asymmetric tilt boundaries of the type {1 0 0}/{4 3 0}. At the positions of the coherent, high coincidence symmetric tilts, {1 2 0}/{1 2 0}, the population reaches a minimum and the energy

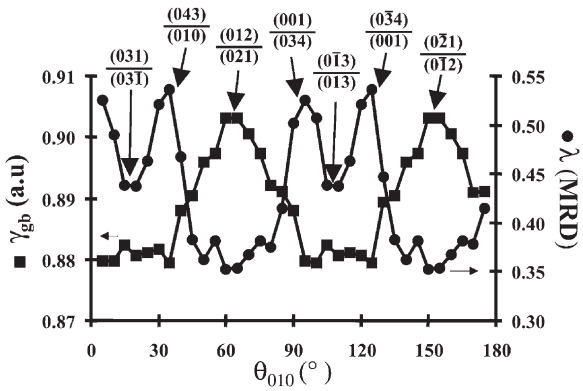

Fig. 7. Comparison of the reconstructed energies (squares) and the observed distribution (circles) for Σ5 tilt boundaries. The quantities are plotted in 5° intervals as a function of the angle between the boundary plane normal and (0 1 0)/(0 4 $\bar{3}$). For reference, the location of the symmetric tilts, both the {3 1 0} and {2 1 0} types, as well as the asymmetric boundaries terminated by {1 0 0} planes are indicated. Note that the function has mirror symmetries at the symmetric tilt orientations, {2 1 0} and {3 1 0}. The deviations from this are due to the relatively large intervals of the plotted points.

reaches a maximum. This indicates that asymmetric boundaries with {1 0 0} planes are favored over the high coincidence boundaries. The other symmetric boundary in this tilt system, which has only partial coincidence, is the {3 1 0}/{3 1 0}. This boundary has an energy similar to the asymmetric {1 0 0}/{4 3 0}, but occurs at a minimum in the population. It should also be noted that the {1 0 0}/{1 0 0} twist boundary (not shown), which also has a high coincidence, does occur at a maximum in the population. However, {1 0 0}/{1 0 0} twist boundaries exhibit high populations and low energies at all <1 0 0> misorientations (see Fig. 6) and we therefore argue that the special nature of this particular boundary derives from its dual {1 0 0} interface plane rather than its particular misorientation.

The observation that grain boundaries with {1 0 0} planes have relatively low energies at all misorientations can be quite simply explained by assuming that the grain boundary energy is proportional to the surface energies of the planes that make up the boundary, which is also proportional to the density of broken bonds on these planes. The dominant influence of broken bond density or free surface characteristics on the grain boundary energy may be surprising in comparison to theories for grain boundary structures based on repeat units that are distinct from arrangements occurring in the bulk or on a free surface [32,33]. However, earlier microscopic studies of Σ5 grain boundaries in bicrystals of the isostructural compound, NiO, are entirely consistent with our conclusions. Merkle and Smith [34] noted that while repeat structures can be located in Σ5 tilt boundaries, they occur only in boundary segments where the symmetric {2 1 0}/{2 1 0} configuration is realized and that asymmetric segments along the same boundaries with the {4 3 0}/{1 0 0} configuration were more common. It is worth noting that the success of studies seeking the properties and structure of low Σ CSLs or repeat units in highly symmetric boundaries does not imply that these interfaces are important, special, or even particularly common interfaces in real polycrystalline microstructures.

The dominance of boundaries with {1 0 0} surface planes and the ability of the surface energy anisotropy to predict the relative energies of grain boundaries is reasonable, since the excess energy of the interface derives from incomplete bonding. The {1 0 0} plane has the highest coordination number (fewest broken bonds) and for the most common case of a general boundary where the surface repeat units in parallel planes on either side of the interface do not form a periodic structure, it is easy to imagine that a relatively low energy would result by fixing one of the planes in the {1 0 0} orientation. The fact that the surface energy is a good predictor of the grain boundary energy must derive from the fact that the amount of energy gained by bringing two surface planes together to form a boundary is more or less constant. Boundary atoms in incommensurate interfaces experience a wide range of possible atomic configurations and this range is not expected to depend strongly on the type of boundary. As long as the details of the atomic relaxations in a specific boundary are as widely varied along the aperiodic structure as they are from boundary to boundary, they average to about the same value. Thus, the surface energies provide a good measure of the density of unsatisfied bonds in the interface and, therefore, the grain boundary energy.

The findings suggest that for MgO, it is possible to create a model for the grain boundary energy based on the knowledge of the dislocation structure and the surface energy anisotropy. Knowing the most prevalent types of dislocations in the system, the five parameter energy distribution can be estimated for low angle boundaries using RS [23] theory, and the surface energy anisotropy can be used to compute the energies of all higher angle boundaries. The generality of such a model is currently not known. It is possible that because of more directional bonding in covalent systems and shorter range forces in metallic materials, the surface energy will not be a reliable predictor of the grain boundary energy in other types of materials. We plan to test this in the future. However, the model has several appealing features. First, the surface energy is only a two parameter function and it is therefore much easier to measure than the five parameter grain boundary function. Second, if the grain boundary energy anisotropy can really be estimated from the energies of the two surfaces that comprise the boundary, then the grain boundary energy is reduced to a function of only four parameters. In other words, the energy for high angle misorientations is independent of rotations about **n**. We note that the approximate independence of the grain boundary energy on the twist angle (when the misorientation axis and **n** are parallel) for high misorientation angle grain boundaries has been observed in Cu [7].

The extended annealing of the sample prior to analysis was intended to ensure local thermodynamic equilibrium at the boundaries. While this paper has focused on the geometry and energies of the boundaries, we assume that chemical equilibrium was also achieved. In other words, we assume that boundaries with the same five macroscopically observable parameters have the same composition. As part of a separate experiment, the composition of this sample has already been studied and the principal impurity is Ca, which is present at a bulk concentration of 0.2% [35]. We are presently surveying grain boundary compositions and preliminary results, based on the analysis of hundreds of boundaries, indicate that Ca segregation is anisotropic and that the most frequently observed boundaries accumulate the least Ca [36].

Perhaps the most exciting outcome of this study is the inverse correlation between the grain boundary energy and the population. If this correlation is a general feature of late stage microstructures, then the direct observation of the grain boundary population will be a good way to estimate the relative grain boundary energy. The correlation implies that as grain growth proceeds, higher energy boundaries are eliminated preferentially so that lower energy boundaries persist and dominate the population. However, the idea that the grain boundary population is refining toward a lower energy can be misleading, since no grain boundaries actually persist throughout the entire grain growth process; whenever a grain disappears, new boundaries appear. For example, as the grain size increases from 1 to 100 μ, only 1 in 10^6 grains survive and the probability that any boundary between two crystals in the initial configuration survives this process is extraordinarily small. The inverse correlation of the population and energy is probably better explained as a kinetic phenomenon. The time that any given grain boundary exists in microstructure is, on average, equal to the time it takes to move through a neighboring grain of average size. High mobility boundaries move through neighbors in a shorter time interval and are, therefore, annihilated more rapidly than low mobility boundaries. Assuming energy and mobility to be correlated, then, at any instant in time, there should be more low energy (mobility) boundaries than high energy (mobility) boundaries.

5. Summary

In the five-dimensional domain of grain boundary types, the boundary energy and population exhibit an inverse correlation. This implies that during grain growth, higher energy boundaries are preferentially eliminated in favor of low energy boundaries. At low misorientation angles, the distribution and energy of the observed grain boundaries can be explained by the conventional Read–Shockley dislocation model. One overarching characteristic of the distribution in MgO is that at all misorientations, the boundaries with {1 0 0} interface planes have relatively low energies and

have higher populations, even in comparison to more symmetric, high coincidence boundaries. By summing the energies of the two surfaces that comprise the boundary, a hypothetical energy function is created that reproduces the inclination dependence of the distribution and energy.

Acknowledgements

This work was supported primarily by the MRSEC program of the National Science Foundation under Award Number DMR-0079996.

References

[1] Goux C. Can Metall Q 1974;13:9.
[2] Smith, C.S., "Grains Phases and Interfaces: an Interpretation of Microstructure," TP 2387 in Metals technology, June 1948.
[3] Hasson GC, Goux C. Scripta Metall 1971;5:889.
[4] Zhukova TI, Fionova LK. Sov Phys Solid State 1983;25:472.
[5] Saylor DM, Morawiec A, Adams BL, Rohrer GS. Interface Sci 2000;8:131.
[6] Duyster J, Stöckhert B. Contrib Mineral Petrol 2001;140:567.
[7] Gjostein NA, Rhines FN. Acta Metall 1959;7:319.
[8] Readey DW, Jech RE. J Am Ceram Soc 1968;51:201.
[9] Hodgson BK, Mykura H. J Mater Sci 1973;8:565.
[10] McLean M. J Mater Sci 1973;8:571.
[11] Dhalenne G, Revcolevschi A, Gervais A. Phys Stat Sol (a) 1979;56:267.
[12] Dhalenne G, Dechamps M, Revcolevschi A. J Am Ceram Soc 1982;65:C11.
[13] Kimura S, Yasuda E, Sakaki M. Yogyo-Kyokai-Shi 1986;94:795.
[14] Otsuki A. Acta Mater 2001;49:1737.
[15] Saylor, D.M., Morawiec, A., Rohrer, G.S., Acta Mater. 2003; doi:1016/S1359-6454(03)00181-2.
[16] Herring C. Surface tension as a motivation for sintering. In: Kingston WE, editor. The physics of powder metallurgy. New York: McGraw Hill; 1951. p. 143.
[17] Morawiec A. Acta Mater 2000;48:3525.
[18] Hoffman DW, Cahn JW. Surface Sci 1972;31:368.
[19] Cahn JW, Hoffman DW. Acta Met 1974;22:1205.
[20] Read WT, Shockley W. Phys Rev 1950;78:275.
[21] Frank FC. The resultant content of dislocations in an arbitrary intercrystalline boundary. In: A Symposium on the Plastic Deformation of Crystalline Solids. Washington (DC): Office of Naval Research; 1950. p. 151.
[22] Read WT, Shockley W. Imperfections in nearly perfect crystals. New York: Wiley, 1952 p. 352.
[23] Dodsworth J, Carter CB, Kohlstedt DL. Formation of grain boundaries in MgO by deformation. In: Yan MF, Heuer AH, editors. Advances in Ceramics, vol. 6. Columbus (OH): American Ceramic Society; 1983. p. 75.
[24] Hirth JP, Lothe J. Theory of dislocations, 2 Malabar, FL: Krieger Publishing company, 1992 p. 282.
[25] Press WH, Flannery BP, Teukolsky SA, Vetterling WT. Numerical Recipies in Pascal. UK: Cambridge University Press, 1989.
[26] Williams F. Reasoning with statistics. Fort Worth: Harcourt Brace Jovanovich, 1992.
[27] Saylor DM, Rohrer GS. Interface Sci 2001;9:35.
[28] Wolf D. J Mater Res 1990;5:1708.
[29] Bollman W. Crystal defects and crystalline interfaces. New York: Springer-Verlag, 1970 p. 143–149.
[30] Randle V. The role of the coincidence site lattice in grain boundary engineering. London: Institute of Materials, 1996.
[31] Chaudhari P, Matthews JW. J Appl Phys 1971;42:1971.
[32] Ashby MF, Spaepen F, Williams S. Acta Metall 1978;26:1647.
[33] Pond RC, Smith DA, Vitek V. Acta Metall 1979;27:235.
[34] Merkle KL, Smith DJ. Ultramicroscopy 1987;22:57.
[35] Saylor DM, Mason DE, Rohrer GS. J Am Ceram Soc 2000;83:1226.
[36] Papillon, F., Wynblatt, P., Rohrer, G.S., unpublished work